Theor. Appl. Climatol. 71, 185–197 (2002)

Theoretical and Applied Climatology

[1] Departamento de Ciências Atmosféricas, Instituto de Astronomia Geofísica e Ciências Atmosféricas, Universidade de São Paulo, São Paulo, Brasil
[2] International Research Institute for Climate Prediction, Palisades, NY, USA

Exploring the impacts of the tropical Pacific SST on the precipitation patterns over South America during ENSO periods

C. A. S. Coelho[1], **C. B. Uvo**[2], and **T. Ambrizzi**[1]

With 6 Figures

Received August 10, 2000
Revised August 22, 2001

Summary

Previous studies on precipitation over South America that strongly support the existence of links between precipitation and SST anomalies in the Pacific Ocean have identified specific regions where the ENSO signal is particularly stronger. Northeast of Brazil and some parts of southern South America are examples of these regions. However, the same attention was not taken to identify which regions in the Central and East Pacific ocean are better correlated with the South America precipitation during extreme ENSO events, and also which are the transition regions of the precipitation signal over South America during these events.

Coincident periods of ENSO events for both SST over the tropical Pacific ocean and monthly precipitation sums from many observational stations over South America were selected and analyzed. Two statistical methods were used for the data analysis: Singular Value Decomposition (SVD) and Simple Linear Correlation (SLC). The SVD results for warmer events in the Pacific corroborate previous ones and also clearly identified a transition region between the drier conditions in the Northeast of Brazil and the wetter conditions in the Southeast/South of Brazil. Transition regions were also determined over Peru and central Amazon. The SLC results indicated that the SST anomalies in the tropical east Pacific ocean has the strongest influence in the South American precipitation during El Niño events. During La Niña events the central area of the Pacific, around 180°, has shown a more significant influence.

1. Introduction

The need for accurate long term precipitation predictions has led to numerous studies of the elements that control inter-annual climate variability. Fluctuations in tropical sea surface temperature (SST), as the ones experienced during El Niño/Southern Oscillation (ENSO) episodes, act as global modulators of climate. Relationships between SSTs in the central-eastern Pacific and precipitation around the world (e.g. Ropelewski and Halpert, 1987) has supported a constant monitoring of SSTs over these regions and a long range forecast based on dynamic models (e.g. Zebiak and Cane, 1987) and statistical schemes (Barnston and Smith, 1996; Graham et al., 1987a,b).

During the El Niño austral summer, in some regions of the tropical Americas, precipitation substantially increases as in Ecuador and Peru (Aceituno, 1988). Enhanced convective activity also leads to intense subsidence over northeast Brazil and Central America which suppresses deep tropical convection and results in precipitation deficits or even droughts (Magaña and Quintanar, 1997; Kousky et al., 1984; Uvo et al., 1998). Over the subtropical and mid-latitude

South America, El Niño austral spring and summers result in enhanced precipitation, especially over Southern Brazil, Northern Argentina and Uruguay (Rao and Hada, 1990; Pisciottano et al., 1994 and Grimm et al., 1998, among others).

Consistent ENSO-precipitation teleconnection patterns were documented by Stoeckenis (1981), Ropelewski and Halpert (1986, 1987 and 1989), Lau and Sheu (1988) and Kiladis and Diaz, (1989). They have used the correlation technique, composites and EOF (Empirical Orthogonal Functions) analyses of global precipitation and have defined important relationships on a global and local scale.

Our present understanding of consistent ENSO relations with precipitation during the southern winter and summer seasons has been summarized in schematic pictures in many studies, for instance, see Fig. 2 from Trenberth et al. (1998) which shows those areas around the world where consistent drier/wetter than normal conditions are observed during ENSO. Indeed, the Trenberth et al. paper provides a thorough review of many important issues involved in determining the response of the extratropical atmosphere to tropical forcing associated with SST. Observations, empirical studies, theory and modeling of the extratropical teleconnections are discussed.

Previous studies on precipitation over South America have strongly supported the existence of links between precipitation and SST anomalies in the Pacific Ocean. They have identified specific regions where the ENSO signal is particularly strong as Northeast Brazil (Kousky et al., 1984; Rao et al., 1986; Uvo et al., 1998) and some parts of southern South America (Rao and Hada, 1990; Ropelewski and Halpert, 1987, 1989; Diaz et al., 1998; and Grimm et al., 1998, 2000). However, to our knowledge, there has been no studies identifying which regions in the Central and East Pacific ocean, during extreme ENSO events, are better correlated with the South America precipitation. Also, since we will consider the South American continent as a whole, without division by specific region, the statistical technique used should emphasize those regions with strong signals in a natural way. In particular, we will be looking for regions where a clear transition of correlation signals can be observed.

We start in section 2 by listing the datasets used in this study. In section 3, we describe the methodology used in support of our search for relationships between anomalies in rainfall and different SST regions. Results of the analyses are presented in section 4, followed by a summary and conclusions in section 5.

2. Data

Monthly precipitation data were provided by the Center for Weather Forecast and Climate Prediction (CPTEC), National Agency for Electrical Energy (ANEEL) and the Brazilian Agricultural Research Corporation (EMBRAPA) from Brazil and the National Climate Data Center (NCDC) and the International Research Institute for Climate Prediction (IRI) from the United States. A quality control analysis for the dataset was previously performed by each institution that provided them. The time series used in this study were from 1970 to 1993.

Stations were selected so that, following Lau and Sheu (1988), only stations with less then 10% missing data were used in the data analysis. This condition assures the statistical analyses will not be influenced by the missing data. Among the chosen stations, missing data were filled using the technique developed by Cressman (1959). This technique relates the missing data with the data of stations around it. The locations of the precipitation stations over South America is shown in Fig. 1. For the analyses of El Niño events, 347 rain stations were selected (Fig. 1a) and for La Niña, 326 (Fig. 1b).

The monthly SST dataset was obtained from the Comprehensive Ocean-Atmosphere Data Set (COADS) (Pan and Oort, 1990). It was selected an area from 10° S to 10° N latitude over the Pacific Ocean extending in longitude from Indonesia to the west coast of South America. The data was interpolated to a 5° (longitude) $\times$ 2° (latitude) rectangular grid. The climatology used was based on the period of 1950 to 1997.

Coincident periods of ENSO events for both SST and precipitation were selected and analyzed. The selection criteria was months when the SST anomalies in the Equatorial Pacific were higher than or equal to $+2\,^\circ$C for El Niño and lower than or equal to $-2\,^\circ$C for La Niña. Based on this criteria, the periods chosen to represent El

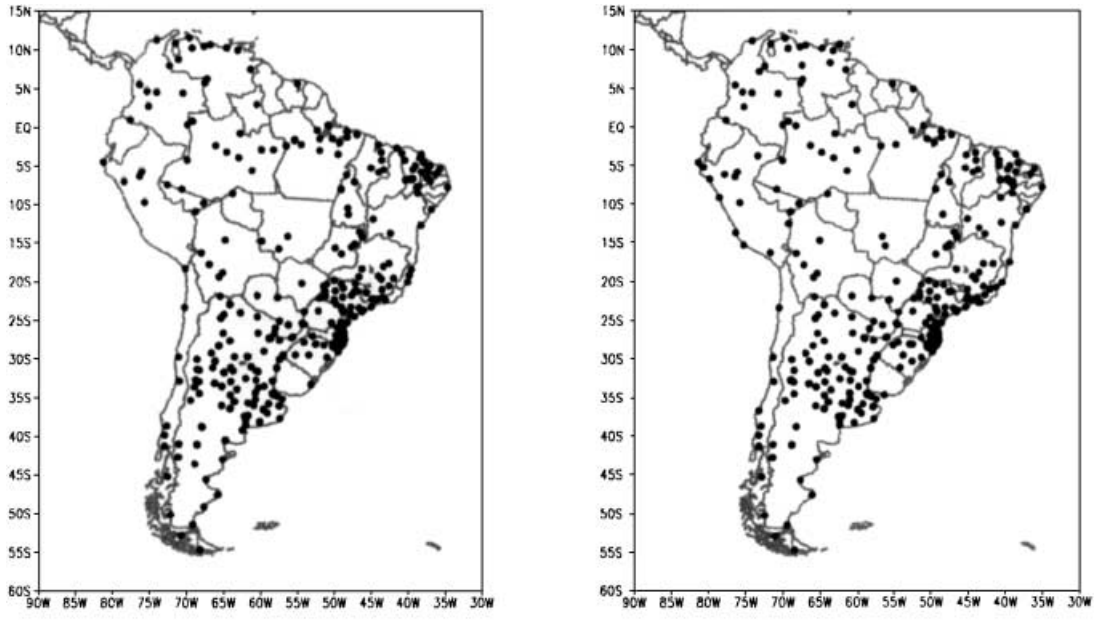

Fig. 1. Location of the rainfall stations used to represent precipitation field over South America during episodes of (**a**) El Niño (347 stations) and (**b**) La Niña (326 stations)

Niño episodes were: March 72 to February 73; May 76 to February 77, May 82 to September 83; and September 86 to December 87. For La Niña episodes, the selected periods were: May 70 to March 71; April 73 to March 74; November 84 to July 85; and May 88 to February 89.

Each of the selected periods were split in 3 sub-sets for further analysis: data from December to May (DECMAY), September to February (SEPFEB), and from periods coincident with the maximum/minimum SST anomaly (MSST). The reason for creating different sub-sets was to better capture the influence of ENSO on precipitation during the rainy season of the northern and northeastern South America (Austral summer and autumn) and southeastern South America (Austral spring) (e.g. Rao and Hada, 1990; Uvo et al., 1998; Grimm et al., 1998).

After this selection, the time series for DECMAY and SEPFEB were composed of 24 time steps for both, El Niño and La Niña, and for MSST of 31 time steps for El Niño and 20 for La Niña. We are conscious that these are not long time series and that statistics with such short time series can be imprecise so we were specially careful in considering only statistically significant results.

Statistical analysis for SEPFEB and MSST have shown low correlation and no statistical significance, therefore only the analysis for the DECMAY period will be presented and discussed here.

3. Methodology

Two methods were used for data analysis in this work and their results were compared. Analyses were made by means of Singular Value Decomposition (SVD) and Simple Linear Correlation (SLC). One may ask why it is necessary to use both SVD and SLC. SVD will give us a general idea of the most important oceanic areas which are better correlated with precipitation over the South American continent. However, to determine which specific oceanic area has the most significant influence on the precipitation, the SLC technique is more appropriated. The description of these two methods is presented in the next two subtopics.

3.1 Singular Value Decomposition (SVD)

SVD isolates linear combinations of variables within two fields that tend to be linearly related

to each other. As result, SVD provides spatial patterns from the two fields that explain most of the covariance between them.

The use of SVD in a meteorological context is quite recent. Prohaska (1976) was the first to use it to document the relationship between two meteorological fields. After that, not many studies using SVD to relate geophysical fields were published until Bretherton et al. (1992) and its companion paper, Wallace et al. (1992). After them the use of SVD for geophysical purposes increased considerably. Some examples of the use of this technique may be found in Wallace et al. (1993), Uvo and Berndtsson (1996) and Uvo et al. (1998). Jackson (1991) and Preisendorfer (1988) present a thorough description of SVD theory and Newman and Sardeshmukh (1995) discussed some of the problems that should be considered when using SVD to recover the relationship between two fields.

3.1.1 The SVD theory

Suppose we have two data sets $Y_{t,y}$ and $Z_{t,z}$ where the subscripts are indicating of time (t) and space (y and z). The time t has *nt* time steps that must be the same for Y and Z. The spatial dimensions y and z have *ny* and *nz* space points that do not need to be the same. Each column of Y and Z must be normalized with zero mean.

SVD finds spatial patterns G and H that are a linear combination from Y and Z, respectively, and explains most of the total covariance between them, i.e.:

$$U = YG; \tag{1}$$

$$V = ZH; \tag{2}$$

We define the cross-covariance matrix of Y and Z as

$$C_{YZ} = \frac{1}{nt-1} Y'Z$$

where Y' is Y transposed.

The patterns G and H are chosen such as the covariance between U and V is maximized. This covariance can be written as:

$$\begin{aligned} \mathrm{cov}(U, V) &= \langle U'V \rangle \\ &= \frac{1}{nt-1} \sum_{t=1,nt} U'_t V_t = \max \end{aligned} \tag{3}$$

Using (1) and (2) in (3) comes:

$$\begin{aligned} \langle U'V \rangle &= \frac{1}{nt-1} G'Y'ZH \\ &= G'C_{YZ}H = \max \end{aligned} \tag{4}$$

The equation system formed by (1) to (4) is the basis for the SVD calculation and must be solved for G and H. The solution for this system is given by:

$$(C'_{YZ}C_{YZ} - \sigma^2 I)G = 0$$

$$(C_{YZ}C'_{YZ} - \sigma^2 I)H = 0$$

where σ^2 are the eigenvalues of $C_{YZ}C_{ZY}$ and G and H the eigenvectors (details of this developments can be found in Uvo and Graham, 1998).

When SVD is applied to the C_{YZ} cross-covariance matrix between two fields – in the present case SST and precipitation – it identifies the pairs of spatial patterns which explain most of the temporal covariance between the two fields.

Each mode resulting from the SVD analysis is composed by a pair of singular vectors (eigenvectors), one for each field that is being analyzed, and a vector of singular values (eigenvalues). For simplification of interpretation, results from the SVD can be analyzed in the form of homogeneous and heterogeneous correlation maps. In this way, each SVD mode generates a pair of heterogeneous and a pair of homogeneous correlation maps. The k^{th} homogeneous map is defined as the vector of correlations between the grid values of one field and the k^{th} mode of the singular vector of the same field. Similarly, the k^{th} heterogeneous correlation map is the vector of correlations between the grid values of one field and the k^{th} mode of the singular vector of the other field. The homogeneous correlation map is an indicator of the geographic localization of covarying parts of the field while the heterogeneous correlation map indicates how well the grid points of one field relate to the k^{th} expansion coefficient of the other.

In this paper, special attention is given to the heterogeneous correlation maps as we seek the influences of SST over precipitation. The correlation coefficient (CC) between the reconstructed times series of both fields at each mode was also calculated.

To determine if the correlation coefficients from the homogeneous or heterogeneous correlation maps differ significantly from what may be expected due to chance, a test of the null hypothesis based on the Student's t distribution can be performed (Bendat and Piersol, 1986). This test is performed considering the autocorrelation of the dataset in order to measure the independence of the time series.

The maximum covariance is equal to the largest singular value, σ_1, and is obtained by projecting one field onto the first singular vector of the same field. The total squared covariance explained by a single pair of patterns is σ_k^2, so that the squared covariance fraction (SCF), i.e., the percentage of the squared covariance explained by the pair of patterns, is:

$$\mathrm{SCF_k} = \frac{\sigma_k^2}{\sum_{l=1}^{\min(nt,nz)} \sigma_l^2}$$

where nt is the number of time steps and nz the number of stations or grid point in the field. The SCF is useful for comparing the relative importance of modes in a given expansion.

3.2 Simple Linear Correlation (SLC)

The area over the Pacific Ocean identified as the area significantly correlated to the precipitation over South America by the SVD was divided into seven sub areas of 15 degrees longitude $\times$ 10 degrees latitude as shown in Fig. 2. The time series of the mean SST anomaly for each of these areas were correlated to the corresponding time series of precipitation anomalies of each station over South America. An example of application of this technique, applied to OLR and global fields of vector wind and geopotential, can be found in Kiladis and Weickmann (1992). This methodology is similar to the one point correlation technique applied by Bjerknes (1969) between sea level pressure at Djakarta, Indonesia, and 200 other locations around the globe.

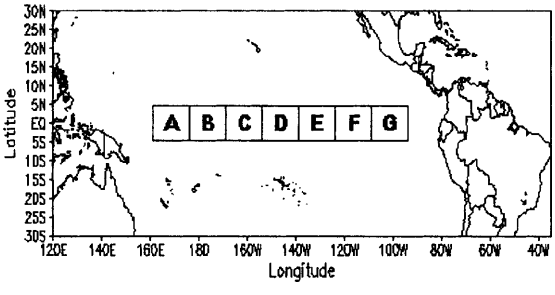

Fig. 2. Regions over the Pacific Ocean used for linear correlation analysis of SST and precipitation

The statistical significance of the correlations was verified by the test of the null hypothesis based on the Student's t distribution (Bendat and Piersol, 1986).

4. Results and discussion

4.1 SVD – El Niño period

Typical precipitation patterns observed over South America during ENSO events were identified during the DECMAY period. Figure 3 shows the heterogeneous correlation maps for the first mode of the SVD analysis between SST anomalies over equatorial Pacific ocean and precipitation anomalies over South America during warm episodes for the period DECMAY. A percentage of 60.6% of the total covariance of the system is explained by this mode and the correlation coefficient (CC) between the reconstructed precipitation and SST time series based only on this mode is equal to $+0.77$.

Note that in the heterogeneous correlation map for precipitation (Fig. 3a) the areas which presented positive correlation coefficients are dark shaded, so that the regions of signal transition become evident. Areas with correlation coefficients higher than $+0.4$ and lower than -0.4 are consistent to a level of significance higher than or equal to 90%. The description presented for Fig. 3a is also valid for Figs. 4a, 5 and 6.

The SST heterogeneous correlation map (Fig. 3b) shows a large region located eastward of 160° W in the equatorial sector, with correlation coefficients up to 0.8 (correlation coefficients higher than 0.4 are statistically significance at $\geq 90\%$). This region is positively and significantly correlated to the precipitation over Ecuador and northern Amazonia and negatively correlated to the precipitation in Northeast Brazil. Therefore, this region can be considered the one which is better related to precipitation over South America during El Niño episodes in DECMAY.

In general, the positive SST anomalies typically observed during El Niño episodes over central-east equatorial Pacific are linearly associated to negative precipitation anomalies over

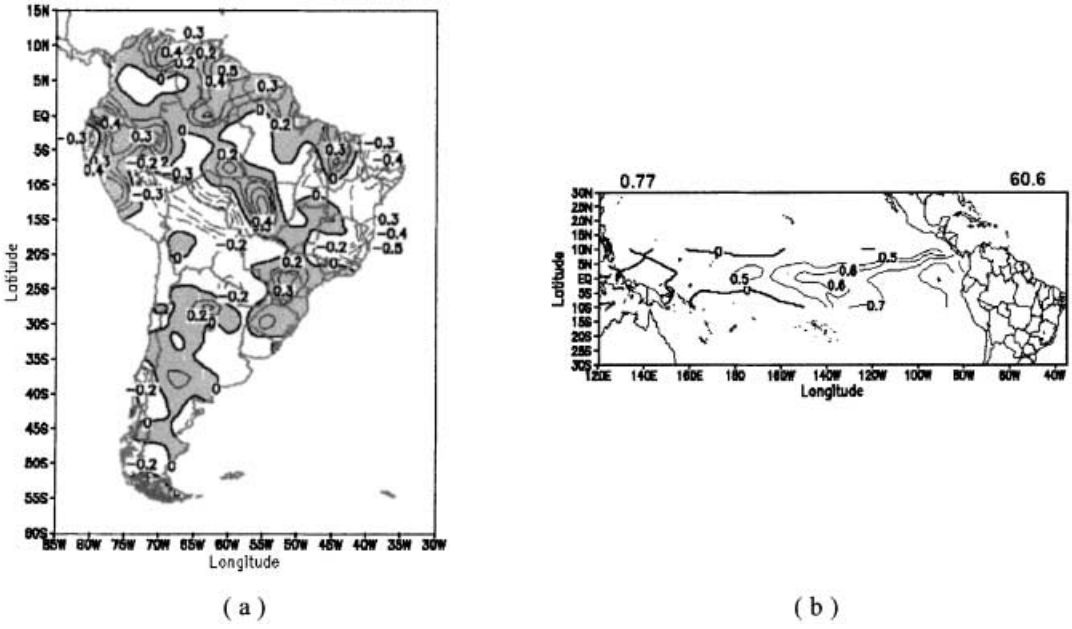

Fig. 3. First mode of the heterogeneous correlation map between (**a**) precipitation and (**b**) SST during December to May of El Niño episodes. The number at the top left of the SST map is the correlation coefficient between the SST and the precipitation expansion coefficients and the one at the top right, the squared covariance fraction of this mode in percentage. Isolines are on 0.1 interval. Dashed (solid) isolines are negative (positive) values. Shaded areas represent regions with positive correlation. Correlation coefficients higher than $+0.4$ and lower than -0.4 are statistically significant at the level higher than or equal to 90%

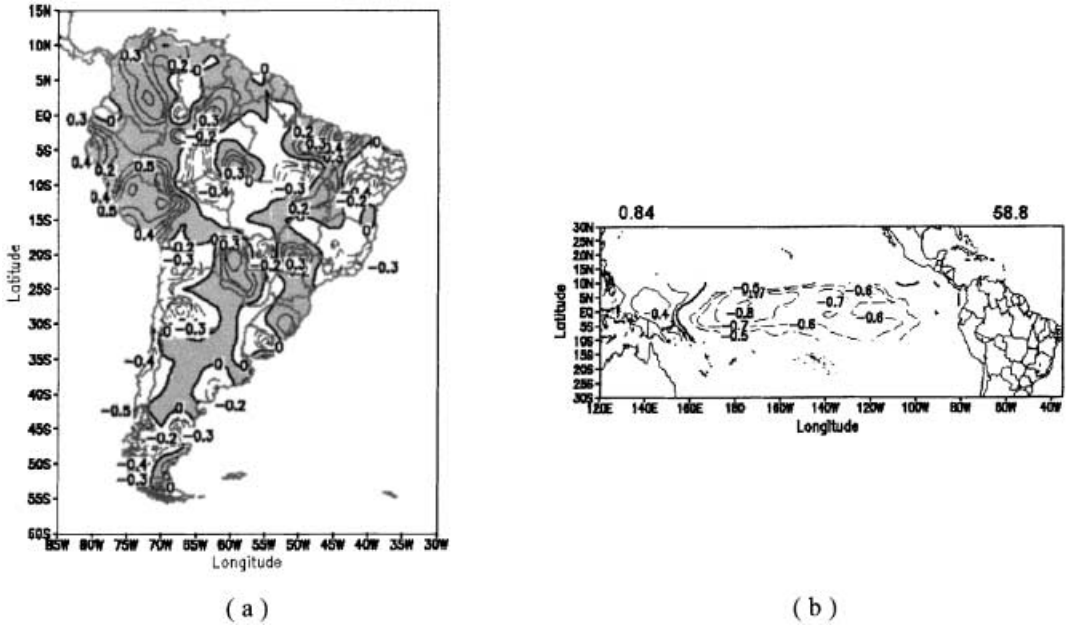

Fig. 4. Same as Fig. 3 but for La Niña episodes

the most part of the northeast region of Brazil and northeastern Bolivia, and positive precipitation anomalies over Peru, Ecuador, Guyana, northern Amazonia, central and southern Brazil and northern Argentina.

As this work seeks to define the limits of the areas of influence of ENSO over South America and the physical causes related to this change of behavior, follows an analyze of the transition regions between the different areas of ENSO

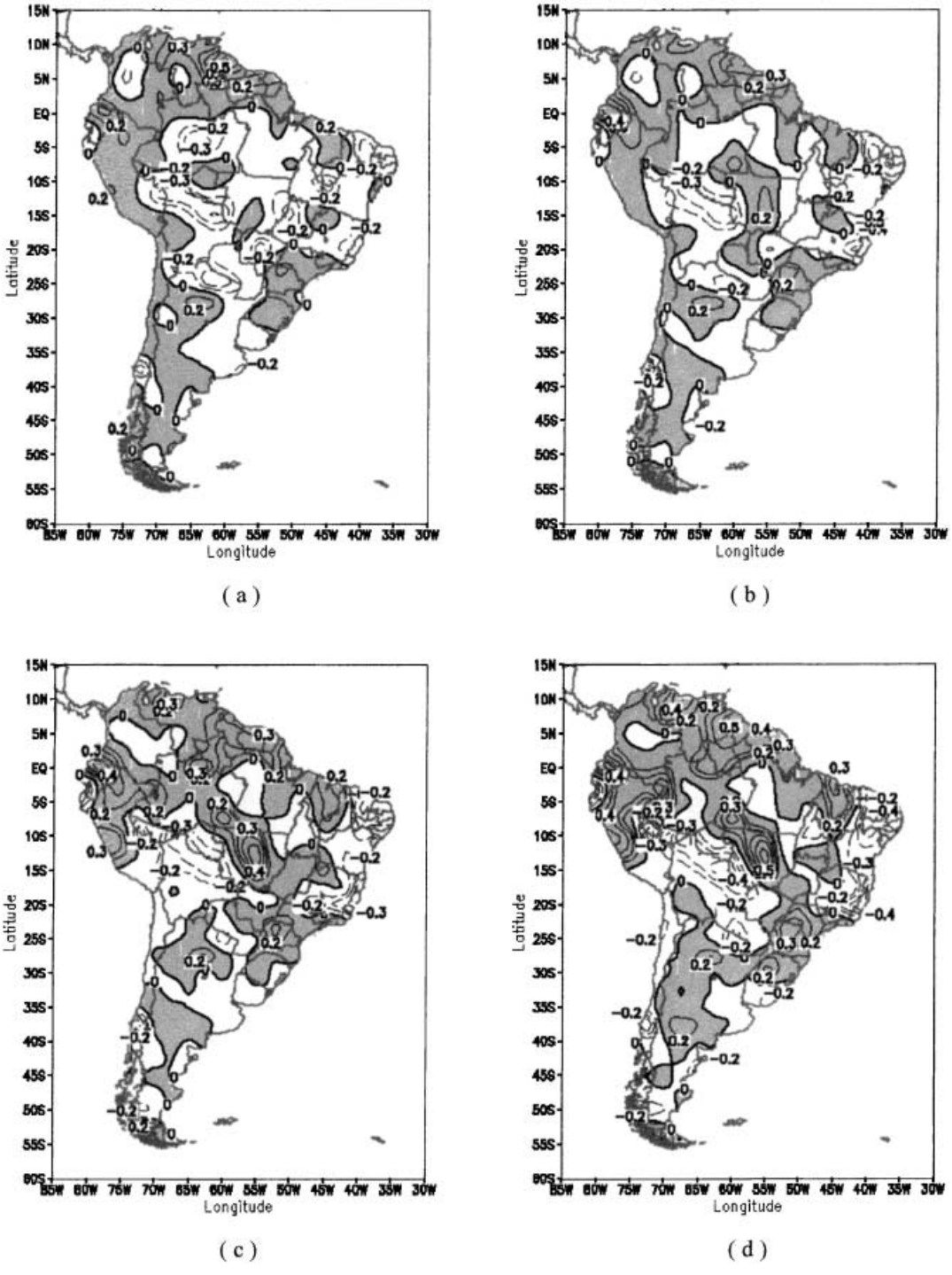

Fig. 5. Correlation maps between precipitation and SST averaged over the areas (**a**) B, (**b**) C, (**c**) E and (**d**) G defined in Fig. 2 during December to May of El Niño episodes. Isolines are on 0.1 interval. Dashed (solid) isolines are negative (positive) values. Shaded areas represent regions with positive correlation. Correlation coefficients higher than $+0.3$ and lower than -0.3 are statistically significant at the level higher than or equal to 90%

influence and speculates about the possible physical mechanisms associated to them.

Through Fig. 3a it is possible to identify the limits of the areas of opposite influences of El Niño over South America. These limits are indicated by three regions of sharp transition between positive and negative correlation coefficients. The first one appears in the northern part

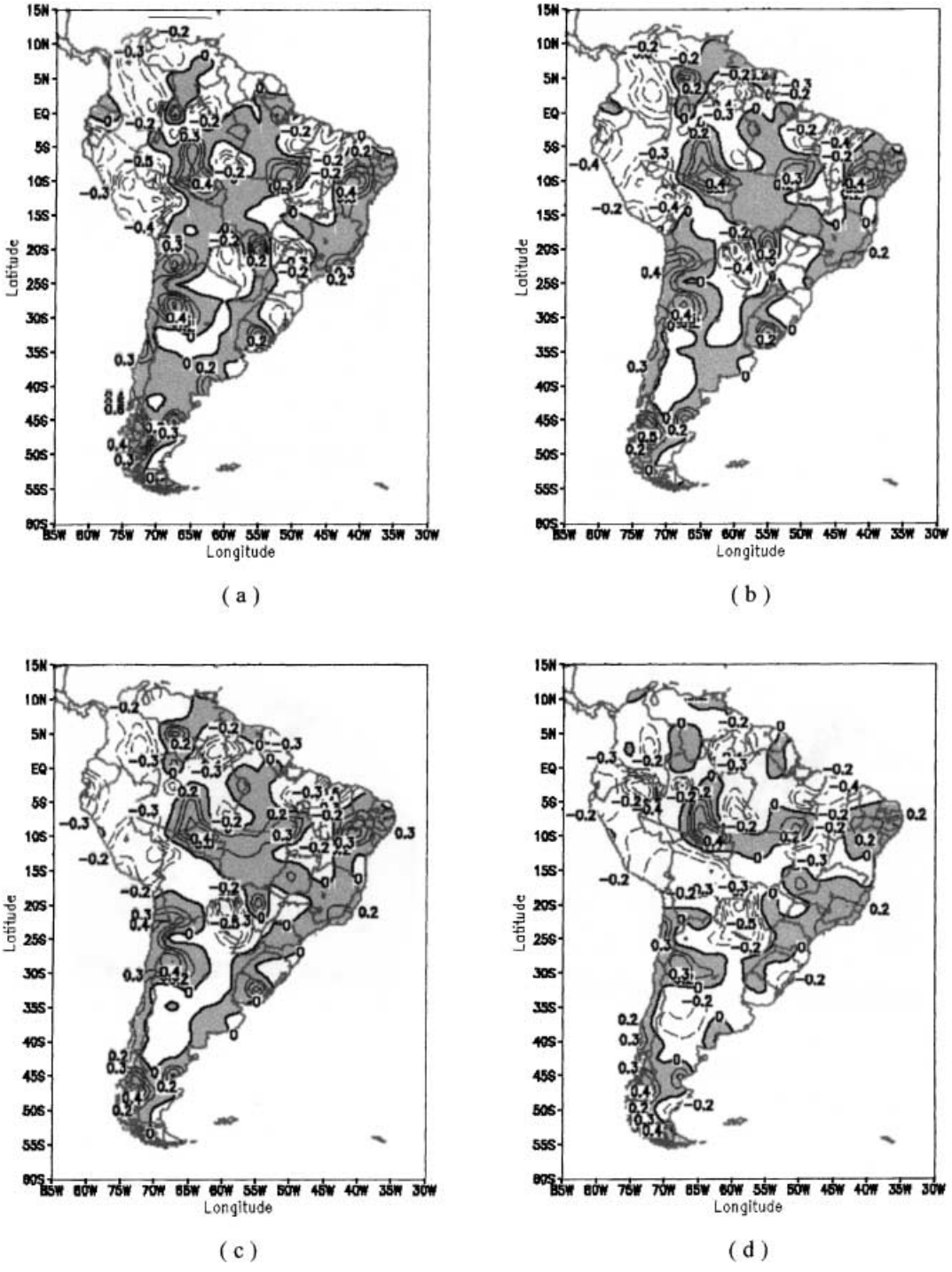

Fig. 6. Same as Fig. 5 but for La Niña and areas (**a**) B, (**b**) E, (**c**) F and (**d**) G. Correlation coefficients higher than $+0.4$ and lower than -0.4 are statistically significant at the level higher than or equal to 90%

of São Paulo State (around 22,5° S) defining the boundary from the drier conditions in the Northeast Brazil and the wetter conditions in the South/Southeast Brazil. The second one is over Peru and shows wetter conditions in the northern Peru and drier conditions over southern Peru and northern Bolivia. Finally the third region is over central Amazonia, splitting wetter conditions in the western Amazon and the drier ones in the eastern Amazon and Northeast Brazil.

The identification of these transition regions are important because around them the precipitation

predictability is reduced when compared with those regions where a single signal is observed. In other words, the ENSO signal over transition regions can be positive or even negative. It will depend on the position of the transition zero isoline. A single displacement of the transition isoline to the north (south) or to the east (west) can alter the ENSO signal around it.

The precipitation anomalies associated with ENSO events may be caused by changes in the water vapor availability, in the dynamics leading to vertical movements, and in the vertical stability of the air, or due to a combination of these factors. In general, humid (dry) anomalies result from the enhancement (weakening) of already existing climatic circulation features that favor (oppose) the precipitation during a giving season in specific regions.

The transition which appears in the northern part of São Paulo and establishes the limits between the different influences of ENSO over northeast and southeast Brazil may be associated with the 200 hPa circulation pattern. It is composed by cyclonic circulation over the South Pacific, anticyclonic to the south/southeast of Southern South America, and cyclonic circulation to the east of Northeast Brazil (not shown). The confluence of these last two circulation patterns coincides with the transition region. In addition, at lower levels, a low pressure system extends up to southeast and central-west regions of Brazil, producing a northwesterly flow over southeast and south regions of Brazil. This flow allows warm and humid advection from the tropical forest. During summer the South Atlantic Convergence Zone (SACZ) is formed over this region (Kodama, 1992, 1993). The SACZ high variability can also have some influence on the definition on the transition region around 22.5° S over northern São Paulo State suggesting that the interaction among these systems determine the limits of the opposite ENSO influences over the east part of South America. Similar analysis have been suggested by Grimm et al. (2000).

A possible explanation for the transition correlation signal over Peru is the mass conservation law. During El Niño events, due to warmer SST over the equatorial Pacific near the coast of Peru, an anomalous convection pattern dominates this region. This convective system produces above normal rainfall over northern Peru and Ecuador while below normal precipitation is observed over southern Peru and northern Bolivia due to compensatory subsidence motion, defining the transition over the center of Peru.

The transition over the center of Amazon that marks the change of behavior of ENSO in this area, is related to changes in the position of the descending branch of the Walker cell in this region. In the northern South America, the variability of the precipitation pattern is mainly due to changes in the zonal thermal Walker circulation in the equatorial region. The displacement of the low level convergence zone from the center of Amazon to the west coast of Peru, observed during El Niño events, leads to an inversion in the zonal circulation cell, with predominance of subsidence over eastern Amazon and northeast region of Brazil and ascending vertical motion over northern Peru, Ecuador and western Amazon.

In particular in regions where the Peruvian and Amazonian transition zones were identified, the few available stations suggest more careful interpretation, specially over the Amazon. Over Peru Aceituno (1988) had already identified opposite correlation signals between the SOI and precipitation in the north and in the south of Peru during November–February.

4.2 SVD – La Niña period

Figure 4 shows the heterogeneous correlation maps for the first mode of the SVD analysis between SST anomalies over equatorial Pacific ocean and precipitation anomalies over South America during cold episodes for the period DECMAY. This mode explains 58.8% of the total covariance of the system and has a CC of $+0.84$. A large region between 160° E and 100° W in the equatorial sector of the Pacific presented correlation coefficients up to -0.8 (Fig. 4b). Correlation coefficients lower than -0.4 are statistically significance at $\geq 90\%$. Comparing both phases of the Southern Oscillation, it seems that during La Niña events the central part of the equatorial Pacific ocean has a more significant influence over the South America precipitation.

Figure 4 shows that the negative SST anomalies observed during La Niña episodes in the

equatorial Pacific ocean are mainly associated to positive anomalies of precipitation in the southern Peru, central region of Colombia, northern Venezuela, Paraguay, South region of Brazil, southern Southeast region of Brazil and some regions of the northeast of Brazil such as southern Bahia, the coast of Piauí and Maranhão. Patterns of negative precipitation anomalies are identified in northwestern Argentina, east and west extremes of the northern parts of Brazil, and in the semiarid region of the Northeast Brazil. However, some care must be taken when considering these results which were reproduced using only the Pacific SST. Recent studies, see for example Pezzi and Cavalcanti (2001), have shown that the Atlantic ocean is also important in determining the precipitation pattern over South America, specially over the northeast region of Brazil.

It is possible to identify through Fig. 4a, four transition regions of correlation coefficients. The first one, as during El Niño events, appears over São Paulo State defining a boundary from the drier than normal conditions on the east Northeast and parts of Southeast Brazil and the wetter conditions to the South. The second one over the center of Bolivia, splits wetter than normal conditions over northern Bolivia and South Peru from drier ones over southern Bolivia and northwestern Argentina. The third transition region lies over the west of the Brazilian Amazonia oriented in the east-west direction, splitting wetter than normal conditions over Peru and drier ones over extreme west Amazon, and the last transition signal region appears over the east of Amazon where we could identify drier than normal conditions in the extreme east Amazon and the wetter ones in the extreme west of the Northeast region of Brazil.

In terms of the high level circulation patterns, there are many similarities when compared with El Niño periods. The South Pacific cyclone, the anticyclone over South of Brazil and the cyclone circulation to the east of Northeast Brazil are still observed (not shown). However, the main position of these last two circulation patterns are slightly different, being to the north in the first one and to the east in the last one. The low level circulation is also similar to that observed during the El Niño period, though the northwesterly low level jet over the south/southeast Brazil shows slightly strong amplitudes. In general, the precipitation anomalies are the result of changes of already existing climatic circulation features that influence the rainfall in specific regions. It seems that during La Niña, the main differences on the precipitation patterns occur due to the weakening of the circulation patterns over South America, such as the subtropical jet, the strengthening of low level jets, and the cyclone and anticyclone positions. A more complete atmospheric circulation study is still necessary to better understand the impact of these differences and the remote response from the equatorial Pacific ocean.

4.3 SLC – El Niño period

The results of the SLC analysis for the warm episodes indicate a poor relationship between SST anomalies over region A (Fig. 2) and precipitation anomalies over South America. On the other hand, results involving the areas B, C, D, E, F and G were similar and showed that the central and eastern sectors of the equatorial Pacific play an important role modulating the precipitation pattern over South America. Figure 5 shows the correlation maps between precipitation over South America and SST anomalies in areas B (Fig. 5a), C (Fig. 5b), E (Fig. 5c) and G (Fig. 5d). Comparing these three figures it is possible to see that area G is the area over the Equatorial Pacific that shows higher correlation with the ENSO precipitation patterns over South America. It is observed that, in agreement with the SVD results, the closer to the continent the higher the influence of the SST over the precipitation.

A closer comparison between results from the SVD and the SLC analyses can be made by comparing Figs. 3a and 5. Both present similar characteristics. Negative correlations are seen over the Northeast and northern Southeast Brazil and northeastern Bolivia. It is observed that areas B and G (Fig. 5a and d) emphasize the signal over northeastern Bolivia. Positive correlations are observed in the northern Peru, Venezuela, central and northern parts of Brazil, northern Argentina and southwestern Bolivia. The transition regions reported in section 4.1 over northern part of São Paulo State (Southeast Brazil), Peru and central Amazon are evident from both methodologies.

4.4 SLC – La Niña period

The results of the SLC analysis for the cold episodes indicate very similar correlation pattern between SST anomalies over regions A to G (Fig. 2) and precipitation anomalies over South America. The areas A, B and C have shown the highest correlation coefficients over South America, and these areas coincide with the region of higher correlation coefficients found in the SVD analysis (Fig. 4b). However, area B have shown the strongest influence over the precipitation in South America in agreement with the region of maximum correlation coefficient found in the SVD analysis (Fig. 4b). Comparing Figs. 4b and 6a it is possible to see a very similar pattern, though, with opposed correlation coefficient signals. It is important to note that, although in both maps only the areas with positive correlation coefficients are shaded, these correlation coefficient maps are showing the same result.

Figure 6 shows the correlation maps between precipitation over South America and SST anomalies in areas B (Fig. 6a), E (Fig. 6b), F (Fig. 6c) and G (Fig. 6d). Figure 6a shows that during La Niña events negative precipitation anomalies can be observed over northwestern Argentina, east and west extremes of the north region of Brazil, as well as in the semiarid region of the Northeast Brazil. Areas E and F emphasize the signal over northwestern Argentina (Fig. 6b and c). Positive precipitation anomalies can be found in some parts of the Northeast of Brazil such as Maranhão and Piauí coast, southern Peru, central and southern Colombia, southern southeast and south regions of Brazil. These results are also in agreement with those obtained through the SVD technique (Fig. 4) described in section 4.2. The four transition regions reported in section 4.2 can also be observed in Fig. 6.

There are many similarities between Fig. 6a, b, c and d. However, a strong signal over Paraguay and extreme east of Bolivia, relating positive precipitation anomalies during La Niña events and negative SST anomalies over equatorial Pacific is emphasized by the correlations between precipitation and SST in areas E, F and G (Fig. 6b, c and d). This positive correlation that indicates a positive precipitation anomaly signal may be related to the intensification of the so called Bolivian High, the thermal driven high level anticyclonic circulation that develops over the region during summer months.

Some correlations between precipitation and the traditional Niño regions (Niño $1+2$, Niño 3, Niño $3+4$ and Niño 4) were also carried out. In general, the results of these correlations were in good agreement with those defined by the boxes areas in Fig. 2. Interesting to remark that during the La Niña events the Niño $1+2$ region did not show any significant signal in the precipitation pattern over South America (not shown). However, when we consider region G, which is just on the left side of Niño $1+2$ region, the South America precipitation pattern was intensified. This result emphasizes the sensitivity of the precipitation over the South American continent with regard to the spatial SST variability in the eastern tropical Pacific.

5. Conclusions

The main relationships between precipitation over South America and SST in the equatorial Pacific ocean during the El Niño and La Niña episodes were identified for the December to May period. Special attention was given to the areas over the Tropical Pacific which SST anomalies most influences precipitation over South America. At the same time, the resulting precipitation pattern over the continent under the influence of ENSO was also carefully examined.

Results showed that SST from different areas of the Equatorial Pacific are related to the precipitation anomalies over the continent during opposite phases of ENSO.

It was identified that the SST anomalies over the central Equatorial Pacific, between 100° W and 150°W, showed to be the region that most strongly influences precipitation in South America during El Niño events. On the other hand, during La Niña events, the central Pacific area, around 180°, has shown to be the most influencing area.

The analysis of the spatial distribution of the precipitation anomalies over South America during El Niño events showed that the precipitation over part of the Northeast Brazil, extreme west of northern Brazil and Bolivia are negatively correlated to the SST, thus experiencing a reduction of precipitation during El Niño episodes. On the other hand, northern Peru, central and southern

Brazil and northern Argentina experience an increase of precipitation during El Niño.

A consistent boundary area between negative and positive influences was observed over the northern part of São Paulo State, around 22,5° S defining the boundary between the Northeast Brazil drier conditions and the South/Southeast wetter ones. Boundary regions also were identified over Peru and central Amazon. The identification of these transition regions are important because around them the precipitation predictability is reduced when compared with those regions where a single signal is observed. In other words, the ENSO signal over transition regions can be positive or even negative. It will depend on the position of the transition zero isoline. A single displacement of the transition isoline to the north (south) or to the east (west) can alter the ENSO signal around it.

For the La Niña episodes, the South American regions associated with positive precipitation anomalies are the central and southern Peru, Colombia, northern Bolivia, Paraguay, South/Southeast Brazil and some parts of the coast of Northeast Brazil. Negative precipitation anomalies related regions are observed over northwestern Argentina, extreme east and west of northern Brazil and the semiarid sector of the Northeast. During the cold events analyses four consistent transition regions were observed. They are on the center of Bolivia, extremes east and west of Amazon and the southeast region of Brazil over São Paulo State.

In general, our results confirm previous ones (Stoeckenius, 1981; Ropelewski and Halpert, 1987; Aceituno, 1988; Rao and Hada, 1990; Diaz et al., 1998; Grimm et al., 2000 and Uvo et al., 1998). In particular, they are consistent to the anomalous precipitation patterns over Brazil and South America obtained by Coelho et al. (1999) and Coelho and Ambrizzi, 2000, in their climatological studies, where the composition technique of ENSO episodes was applied. To previous works, the present one increments a study of the spatial influence of the Equatorial Pacific SST over the South American precipitation and indicates regions of transition between opposite effects in precipitation (dry/wet) over South America during ENSO events.

In this study, we have used linear statistical techniques, which are not able to capture non-linear physical process involved in the dynamical coupled system between ocean and atmosphere. This statistical limitation must be kept in mind during the interpretation of the results. ENSO events show a great variability which are probably associated to non-linear process (Hoerling et al., 1997). Future studies, using non-linear techniques, will be necessary for a better understanding of the ENSO mechanisms and its regional effects.

Acknowledgements

Thanks are due to Dr. Antonio Divino Moura, Dr. Elson Silva and also to the Center for Weather Forecast and Climate Prediction (CPTEC/INPE), the National Agency for Electrical Energy (ANEEL) and the Brazilian Agricultural Research Corporation (EMBRAPA) from Brazil, and the National Climate Data Center (NCDC) and the International Research Institute for Climate Prediction (IRI) from the United States for kindly supplying the rainfall data used in this research. CASC and TA were supported during the development of this work by Fundação de Amparo à Pesquisa do Estado de São Paulo (FAPESP), under processes number 98/15258-1 and 98/12976-0, respectively. TA has also received the support from CNPq (Proc. No. 301111/93-6). CBU was on leave from the Department of Water Resources Engineering, Lund University, Sweden at IRI under the UCAR Visiting Scientist Programs. "Ake and Greta Lissheds Foundation" partially supported CBU during the development of this work. CBU thanks also the Swedish Natural Science Research Council.

References

Aceituno P (1988) On the functioning of the Southern Oscillation in the South America Sector Part I: Surface Climate. Mon Wea Rev 116: 505–524

Barnston AG, Smith TM (1996) Specification and prediction of global surface temperature and precipitation from global SST using CCA. J Climate 9: 2660–2697

Bendat JS, Piersol AG (1986) Random data – analysis and measurement procedures. New York: John Wiley, 525 pp

Bjerknes J (1969) Atmospheric teleconnections from the equatorial Pacific. Mon Wea Rev 97: 163–172

Bretherton CS, Smith C, Wallace JM (1992) An intercomparison of methods for finding coupled patterns on climate data. J Climate 5: 541–560

Coelho CAS, Drumond ARM, Ambrizzi T, Sampaio G (1999) Estudo Climatológico Sazonal da Precipitação sobre o Brasil em Episódios Extremos da Oscilação Sul. Revista Brasileira de Meteorologia 14(1): 49–65

Coelho CAS, Ambrizzi T (2000) Climatological studies of the influences of El Niño Southern Oscillation events in the precipitation pattern over South America during austral summer. Sixth International Conference on Southern Hemisphere Meteorology and Oceanography 1: 149–150

Cressman GP (1959) An operational objective analysis system. Mon Wea Rev 87(10): 367–374

Diaz AF, Studzinski CD, Mechoso CR (1998) Relationships between Precipitation Anomalies in Uruguay and Southern Brazil and Sea Surface Temperature in Pacific and Atlantic Oceans. Bull. Amer Meteor Soc 11: 251–271

Graham NE, Michaelsen J, Barnett TP (1987a) Investigations of the El Niño Southern Oscillation with statistical models. 1: Predictor field characteristics. J Geophys Res 92: 14251–14270

Graham NE, Michaelsen J, Barnett TP (1987b) Investigations of the El Niño Southern Oscillation with statistical models. 2: Model results. J Geophys Res 92: 14271–14290

Grimm AM, Ferraz SET, Gomes J (1998) Precipitation anomalies in southern Brazil associated with El Niño and La Niña events. J Climate 11: 2863–2880

Grimm AM, Barros VR, Doyle ME (2000) Climate variability in Southern South America associated with El Niño and La Niña events. J Climate 13(1): 35–58

Hoerling MP, Kumar A, Zhong M (1997) El Niño, La Niña, and the nonlinearity of their teleconnections. J Climate 10: 1769–1786

Jackson JE (1991) A user's guide to principal components. New York: John Wiley & Sons, 569 pp

Kiladis GN, Diaz HF (1989) Global climatic anomalies associated with extremes in the Southern Oscillation. J Climate 2: 1069–1090

Kiladis GN, Weickmann KM (1992) Circulation anomalies associated with tropical; convection during northern winter. Mon Wea Rev 120: 1900–1923

Kodama Y-M (1992) Large-scale common features of sub-tropical precipitation zones (the Baiu Frontal Zone, the SPCZ, and the SACZ). Part I: characteristics of subtropical frontal zones. J Meteor Soc Japan 70: 813–835

Kodama Y-M (1993) Large-scale common features of subtropical precipitation zones (the Baiu Frontal Zone, the SPCZ, and the SACZ). Part II: Conditions of the circulations for generating the STCZs. J Meteor Soc Japan 71: 581–610

Kousky VE, Kagano MT, Cavalcanti IFA (1984) A review of the Southern Oscillation: oceanic-atmospheric circulation changes and related rainfall anomalies. Tellus 36A: 490–504

Lau KH, Sheu PJ (1988) Annual cycle, quase-biennual oscillation, and Southern Oscillation in global precipitation. J Geophys Res 93: 10975–10988

Magaña-Rueda VO, Quintanar AI (1997) On the use of a general circulation model to study regional climate. 2nd UNAM-CRAY Supercomputing Conference on Earth Science. Mexico City. Numerical Simulations in the environmental and Earth Sciences. Ed. Cambridge University Press, 39–48

Newman M, Sardeshmukh PD (1995) A caveat concerning singular value decomposition. J Climate 8: 352–360

Pan YH, Oort AH (1990) Correlation analyses between sea surface temperature anomalies in the Eastern Equatorial Pacific and the World Ocean. Clim Dyn 4: 191–205

Pezzi LP, Cavalcanti IFA (2001) The relative importance of ENSO and tropical Atlantic sea surface temperature anomalies for seasonal precipitation over South America: a numerical study. Clim Dyn 17: 205–212

Pisciottano GJ, Diaz AF, Cazes G, Mechoso CR (1994) El Niño-Southern Oscillation impact on rainfall in Uruguay. J Climate 7: 1286–1302

Preisendorfer RW (1988) Principal component analysis in meteorology and oceanography. In: Mobley C (ed) Elsevier, 418 pp

Prohaska J (1976) A technique for analyzing the linear relationships between two meteorological fields. Mon Wea Rev 104: 1345–1353

Rao VB, Hada K (1990) Characteristics of rainfall over Brazil: Annual variations and connections with Southern Oscillation. Theor Appl Climatol 42: 81–91

Rao VB, Satiamurti P, Brito JIB (1986) On the 1983 drought in Northeast Brazil. Int J Climatol 6(1): 43–51

Ropelewski CF, Halpert MS (1986) North American precipitation and temperature associated with the El Niño Southern Oscillation (ENSO). Mon Wea Rev 114: 2352–2362

Ropelewski CF, Halpert MS (1987) Global and regional scale precipitation patterns associated with El Niño/ Southern Oscillation. Mon Wea Rev 115: 1606–1626

Ropelewski CF, Halpert MS (1989) Precipitation patterns associated with high index phase of Southern Oscillation. J Climate 2: 268–284

Stoeckenius T (1981) Interannual variations of tropical precipitation patterns. Mon Wea Rev 109: 1233–1247

Trenberth KE, Branstator GW, Karoly D, Kumar A, Lau NC, Ropelewski C (1998) Progress during TOGA in understanding and modeling global teleconnections associated with tropical sea surface temperatures. J Geophys Res 103(C7): 14291–14324

Uvo CRB, Graham NE (1998) Seasonal runoff forecast for northern South America: A statistical model. Water Resources Research 34(12): 3515–3524

Uvo CRB, Repelli CA, Zebiak SE, Kushnir Y (1998) The relationships between Tropical Pacific and Atlantic SST and northeast Brazil monthly precipitation. J Climate 11: 551–562

Uvo CRB, Berndtsson R (1996) Regionalization and spatial properties of Ceará State rainfall in northeast Brazil. J Geophys Res 101(D2): 4221–4233

Wallace JM, Smith C, Bretherton CS (1992) Singular-value decomposition of sea surface temperature and 500-mb height anomalies. J Climate 5: 561–576

Wallace JM, Zhang Y, Lau K-H (1993) Structure and seasonality of interannual and interdecadal variability of the geopotential height and temperature fields in the Northern Hemisphere Troposphere. J Climate 6: 2063–2082

Zebiak SE, Cane MA (1987) A model El Niño-Southern Oscillation. Mon Wea Rev 115: 2262–2278

Authors' addresses: C. A. S. Coelho and T. Ambrizzi, Departamento de Ciências Atmosféricas, Instituto Astronomia, Geofísica e Ciencias Atmosféricas, Universidade de São Paulo, São Paulo, Brazil. Rua do Matão, 1226, Cidade Universitária, CEP 05508-900. (E-mail: cacoelho@model.iag.usp.br and ambrizzi@model.iag.usp.br); C. B. Uvo, International Research Institute for Climate Prediction, LDEO, 61 Rt 9W, Palisades, NY 10964-8000, USA (E-mail: cintia@iri.ldeo.columbia.edu).